






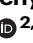


Dopaminergic modulation and dosage effects on brain state dynamics and working memory component processes in Parkinson's disease

Received: 19 January 2024

Accepted: 22 January 2025

Published online: 11 March 2025

 Check for updates


Byeongwook Lee ^{1,6} , Christina B. Young ^{2,6}, Weidong Cai ^{1,3}, Rui Yuan¹, Sephira Ryman², Jeehyun Kim², Laurice Yang², Victor W. Henderson ^{2,3,4}, Kathleen L. Poston ^{2,3,5} & Vinod Menon ^{1,2,3} 

Parkinson's disease (PD) is primarily diagnosed through its characteristic motor deficits, yet it also encompasses progressive cognitive impairments that profoundly affect quality of life. While dopaminergic medications are routinely prescribed to manage motor symptoms in PD, their influence extends to cognitive functions as well. Here we investigate how dopaminergic medication influences aberrant brain circuit dynamics associated with encoding, maintenance and retrieval working memory (WM) task-phases processes. PD participants, both on and off dopaminergic medication, and healthy controls, performed a Sternberg WM task during fMRI scanning. We employ a Bayesian state-space computational model to delineate brain state dynamics related to different task phases. Importantly, a within-subject design allows us to examine individual differences in the effects of dopaminergic medication on brain circuit dynamics and task performance. We find that dopaminergic medication alters connectivity within prefrontal-basal ganglia-thalamic circuits, with changes correlating with enhanced task performance. Dopaminergic medication also restores engagement of task-phase-specific brain states, enhancing task performance. Critically, we identify an “inverted-U-shaped” relationship between medication dosage, brain state dynamics, and task performance. Our study provides valuable insights into the dynamic neural mechanisms underlying individual differences in dopamine treatment response in PD, paving the way for more personalized therapeutic strategies.

Parkinson's disease (PD) is a highly prevalent neurodegenerative disease, affecting more than 1% of adults aged 65 years and older¹. PD is marked by the progressive deterioration of dopaminergic neurons in the substantia nigra², leading to defining motor symptoms, including

tremor, rigidity, and bradykinesia^{3,4}. However, PD is not merely confined to motor disturbances; cognitive impairments are also prominent⁵. While dopamine replacement therapy is widely used to alleviate motor symptoms⁶, dopamine also plays a pivotal role in

¹Department of Psychiatry and Behavioral Sciences, Stanford University School of Medicine, Stanford, CA, USA. ²Department of Neurology & Neurological Sciences, Stanford University School of Medicine, Stanford, CA, USA. ³Wu Tsai Neurosciences Institute, Stanford University School of Medicine, Stanford, CA, USA. ⁴Department of Epidemiology & Population Health, Stanford University School of Medicine, Stanford, CA, USA. ⁵Department of Neurosurgery, Stanford University School of Medicine, Stanford, CA, USA. ⁶These authors contributed equally: Byeongwook Lee, Christina B. Young.

 e-mail: bwlee89@stanford.edu; menon@stanford.edu

cognitive functions, including dynamic, context-dependent, working memory processes^{7–9}. Despite this, our understanding of how dopaminergic medication alters brain circuits associated with distributed cortical-basal ganglia networks that support cognitive functioning in individual PD patients remains poorly understood. Here, we employ computational methods and a systems neuroscience approach to investigate how dopaminergic medication modulates dynamic neural circuits during working memory in PD patients. We also examine how these neural circuit changes relate to individual differences in medication-induced changes in cognitive performance. By doing so, we sought to shed light on the impact of dopaminergic medication on cognitive functions in PD, providing a more nuanced understanding that could potentially guide personalized treatment strategies.

Dopamine deficiency is a major cause of motor and non-motor symptoms associated with PD¹⁰. Optimal cognitive functioning, including working memory, depends on balanced dopamine activity and level^{11–14}. The relationship between brain dopamine and cognitive task performance is complex as dopamine can enhance or impair cognitive control depending on the context and the task¹⁵. In PD, there is a large amount of individual variability in how dopaminergic drugs affect cognition^{15–17}. One likely reason for this variability is that, at the molecular level, the dopamine system is highly dynamic and self-regulates to maintain equilibrium¹⁵. However, how such variability manifests at the systems level in terms of latent dynamic brain circuits engaged during cognition and their medication dosage-dependent modulation in PD is not known. Understanding neural mechanisms underlying complex relationships between dopamine and cognition is crucial for determining optimal dopamine treatment regimens for PD. In this study, we probe into how dopaminergic medication influences the engagement of dynamic brain states during working memory, and examine the impact of the levodopa equivalent daily dosage (LEDD), a standard clinical measure of overall dopamine medication burden in PD.

Working memory serves as an essential component of executive functioning, and is frequently compromised in PD^{18–20}, leading to diminished ability to temporarily hold and manipulate information^{21–23}. Working memory involves a widely distributed cortical-subcortical system, including dorsolateral prefrontal cortex (DLPFC), dorsomedial prefrontal cortex (DMPFC), anterior insula (AI), posterior parietal cortex (PPC), caudate (Cau) and thalamus^{22–27}, and abnormal brain activity and connectivity have been observed in this same cortical-subcortical system in PD patients compared to healthy controls (HC)^{28–31}. However, our understanding of the influence of dopaminergic medication on context-dependent dynamic brain connectivity involving aforementioned regions, integral to working memory functioning, remains limited.

Emerging models of brain circuit dynamics suggest that flexible cognition relies on context-dependent engagement of task-optimal brain states and disengagement of sub-optimal states^{26,27,32–35}. This dynamic framework is especially important for understanding working memory abnormalities, as our previous research indicates a strong relation between working memory performance and the ability to maintain optimal brain states^{26,27}. Accordingly, analysis of irregularities in fluctuating brain states, along with the impact of dopaminergic medication on dynamic brain state engagement during working memory, holds significant promise for deepening our understanding of the neural circuit mechanisms that drive individual differences in levodopa treatment response in PD.

Our study addressed four key objectives (Fig. 1). Our first objective was to investigate dynamic brain states during the three phases of the Sternberg working memory task—encoding, maintenance, and retrieval—in participants with PD³⁶ (Fig. 1A, B), and to assess how dopaminergic medication alters spatiotemporal brain state dynamics (Fig. 1C). Brain states reflect the transient, complex coordination of neural networks that support cognitive subprocesses. By examining

these states, we sought to gain valuable insights into the dynamic interactions between distinct brain regions, capturing rapid shifts in network organization^{26,27}. Such temporal fluctuations are often overlooked by traditional static connectivity analyses, including causal connectivity analysis¹⁷, which limits the understanding of how neural circuits adapt to cognitive demands.

Our second objective was to determine the association between dopamine-mediated alterations in brain state dynamics and individual differences in task performance among PD participants (Fig. 1C, D). We hypothesized that alterations in the temporal properties of brain states would parallel changes in behavioral performance associated with dopaminergic medication.

Our third objective was to determine whether dopamine-mediated changes in behavioral performance on the Sternberg working memory task are associated with brain state-specific dynamic brain connectivity (Fig. 1C, D). We hypothesized that changes in frontoparietal-basal ganglia connectivity would underlie dopamine-related modifications in task performance.

Our final objective was to determine the relationship between dopaminergic medication dosage, changes in spatiotemporal brain state dynamics, and task performance (Fig. 1D). We hypothesized that medication dosage would account for the diverse profiles of individual differences in brain state dynamics and cognitive functioning observed within the PD group.

A total of sixty-four PD and HC participants performed a modified Sternberg working memory task (see *Materials and Methods* for details) during functional MRI (fMRI) scanning (Figs. 1A and 2A). Each PD participant performed the Sternberg working memory task and MRI scanning in both ON and OFF medication sessions in a within-subject design, which allowed participants to serve as their own controls. Each trial of the Sternberg working memory task involved one of three conditions—low-load (LL), high-load (HL), or distractor-load (DL) and was divided into three distinct phases: encoding, maintenance, and retrieval. This experimental design offers an ideal paradigm for investigating the dynamics of brain states and their modulation by cognitive demands and allowed us to probe the effects of dopaminergic medication on dynamics of brain state underlying working memory subprocesses and their relationship to task performance.

We employed a state-of-the-art Bayesian Switching Dynamic System (BSDS) model, which utilizes an unsupervised learning algorithm to identify and track dynamics of brain states at the sub-second scale (Fig. 1B)²⁶. This approach overcomes limitations of conventional methods that impose rigid temporal boundaries linked to predefined task conditions or rely on arbitrary moving windows^{37,38}. Increasingly, such models are being used to uncover meaningful latent variables underlying fMRI and neural recordings^{26,27,39–41}. In the BSDS model, each brain state corresponds to a distinct dynamic process, capturing fluctuations in activation and functional connectivity within an optimal latent subspace. Crucially, this model can not only capture temporal dynamics of brain states but also links them to different phases of working memory, revealing their occurrence rates and the evolving changes in functional connectivity²⁶. We analyzed the occupancy rates of each brain state associated with the encoding, maintenance, and retrieval phases of the Sternberg working memory tasks across varying cognitive load conditions. We hypothesized that dopaminergic medication would remediate aberrant brain state dynamics observed in PD patients.

Utilizing cutting-edge computational modeling, our study elucidates aberrant dynamics of brain states that underpin working memory in PD. Crucially, we uncover the strong influence of dopaminergic medication and dosage on brain state dynamics and its relation to cognitive performance. Our findings provide valuable insights into variability in cognitive performance among PD patients in response to dopaminergic treatment, potentially illuminating pathways for personalized therapeutic strategies for patients.

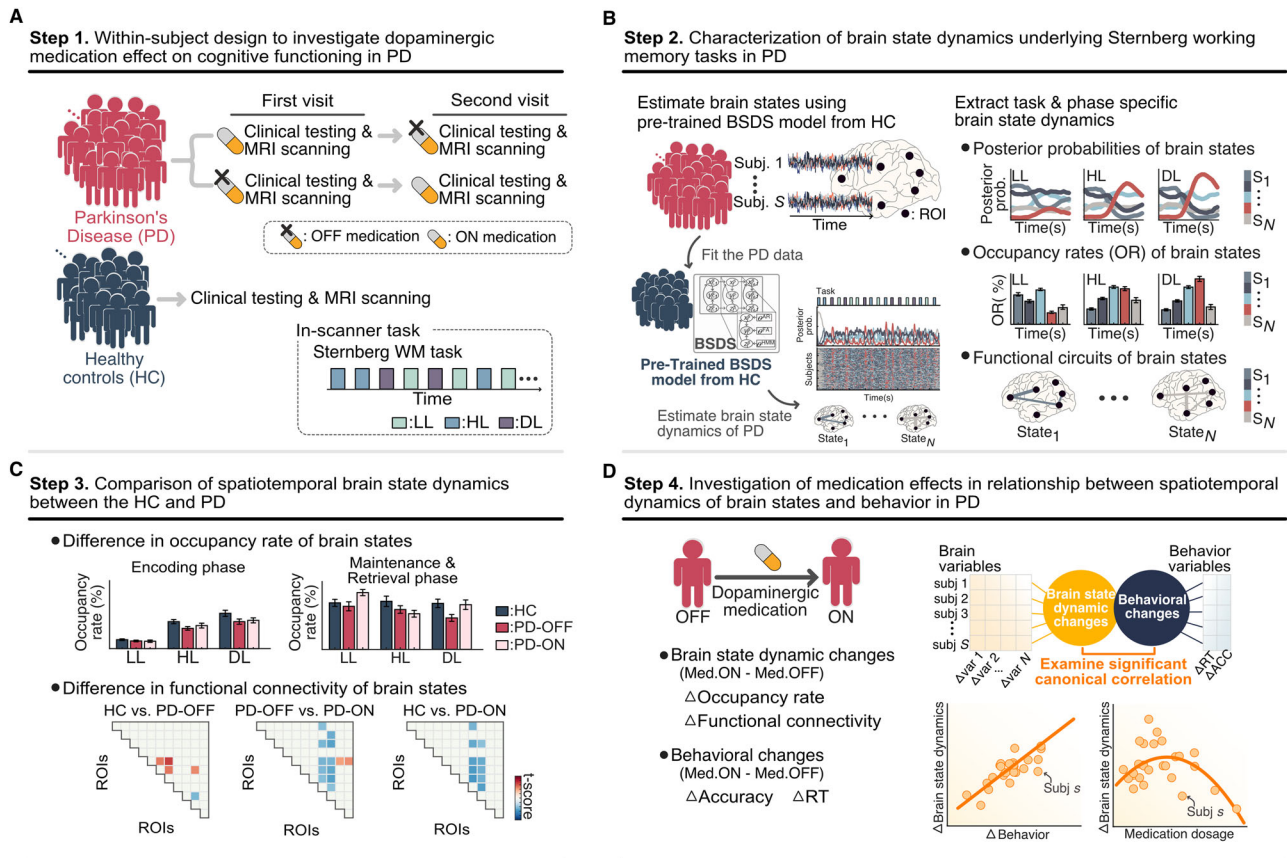


Fig. 1 | Schematic illustration showing overall analysis approach for identifying brain state dynamics in Parkinson's disease (PD). Our approach is composed of four analysis steps. **A** In Step 1, we used within-subject study design to investigate dopaminergic medication effect on cognitive functioning in PD. Each PD participant had two visits, one while during OFF medication (PD-OFF) and the other while ON medication (PD-ON). During each visit, PD participants underwent clinical testing and MRI scanning with performance on a Sternberg working memory (WM) task, which was designed with three levels of difficulty: low-load (LL), high-load (HL), and distractor-load (DL). **B** In Step 2, we used Bayesian switching dynamical systems (BSDS) model to determine the evolution of dynamic brain states underlying the Sternberg WM task in PD participants. A BSDS model trained on healthy

control (HC) data was used to fit PD data and characterize dynamic spatiotemporal properties of brain states ($S_1 \dots S_N$), including (1) posterior probability, (2) occupancy rate (OR), and (3) functional circuit associated with each brain state. **C** In Step 3, we compared spatiotemporal brain state dynamics, including task- and phase-specific occupancy rates and functional connectivity pattern of brain states, in the HC and the PD. **D** In step 4, we investigated whether dopaminergic medication affects brain state dynamics and behaviors in PD group. We examined the relation between changes in spatiotemporal properties of brain states and changes in behavioral performance in PD participants. Finally, we determined whether changes in brain state dynamics and behavioral scores are associated with dopaminergic medication dosage in PD group.

Results

Working memory performance in the PD patients ON and OFF medication

The PD and HC groups were matched for age, sex, and education (Table 1). Analysis of accuracy and RT on the modified Sternberg working memory task confirmed increased task difficulty of the HL and DL conditions in comparison to the LL condition in both HC and PD groups (Fig. 2B and Table 1 and Supplementary Result). There were no significant differences in task performance, both in accuracy and RT, under all three load conditions between the PD-OFF and HC groups, and also between the PD-OFF and PD-ON groups (Fig. 2B, Table 1 and Supplementary Result). Together, these results suggest that both the HC and PD groups exhibited adequate task engagement and performance at the group level.

State-space modeling of brain states associated with Sternberg working memory task performance

We applied state-space modeling using BSDS to cortical-subcortical regions of interests (ROIs), all of which demonstrated task-load effects in our previous study²⁷; each of these regions has been extensively implicated in a range of working memory tasks^{24,42,43} (Fig. 2C). The ROIs include bilateral PPC, DLPFC, DMPFC, anterior insula (AI),

caudate (Cau), and thalamus. BSDS estimated the dynamic spatiotemporal properties of brain states associated with working memory in the PD and HC groups, and we examined effects of PD and dopaminergic medication on brain state dynamics. We identified five brain states and calculated the posterior probability of each brain state at every time point for each PD participant (Fig. 3A, middle). The state with the highest posterior probability was designated as the dominant state at each time point for that participant (Fig. 3A, bottom).

Dynamic temporal properties of brain states associated with Sternberg working memory task performance

We probed the dynamic evolution of brain states during the Sternberg working memory task in PD and HC groups. Our analysis revealed distinct moment-by-moment changes in the posterior probability of brain states across task phases and conditions in both the PD and HC groups (Fig. 3B–D and Supplementary Fig. 3). Notably, the posterior probability of State 1 was highest among brain states during the encoding phase in every task condition and then gradually diminished during subsequent phases in PD and HC groups. In contrast, the posterior probability of State 4 increased during the maintenance phase and peaked in the retrieval phase. These results suggest that State 1 is

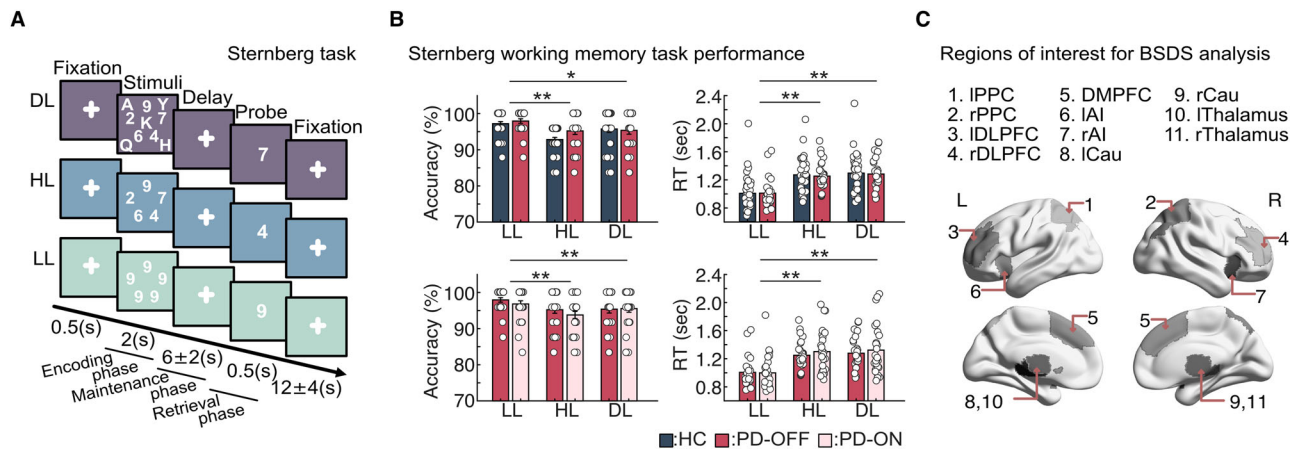


Fig. 2 | Behavioral performance in healthy controls (HC) and Parkinson disease (PD) patients on the Sternberg working memory task. **A** Sternberg working memory paradigm with low-load (LL; 5 identical numbers), high-load (HL; 5 different numbers), and distractor-load (DL; 5 different numbers and 5 different letters) conditions. Each trial consisted of fixation (0.5 s) with stimuli presentation, a maintenance phase (6 ± 2 s) during which a fixation cross is displayed, the presentation of a probe (0.5 s), and an intertrial interval (12 ± 4 s). During the probe, participants indicated whether the probe matched any number displayed during the encoding phase. **B** Accuracy and reaction time (RT) for the Sternberg working memory task across HC, PD-OFF, and PD-ON groups. Accuracy

and RT were significantly greater and faster, respectively, in the LL compared to HL and DL conditions, for all three groups. However, no significant group difference was found in both accuracy and RT for all task conditions. Data are presented as mean values ± SEM. * $p < 0.05$, ** $p < 0.001$. p -values were determined by two-tailed t -test, with FDR correction, $n_{\text{HC}} = 37$, $n_{\text{PD}} = 27$; all exact p -values are provided in Source Data. Source data are provided as a Source Data file. **C** Brain regions of interest (ROIs) used in BDS analysis, which are determined by activation associated with a strong load effect. The ROIs include bilateral posterior parietal cortex (PPC), dorsolateral prefrontal cortex (DLPFC), dorsomedial prefrontal cortex (DMPFC), anterior insula (AI), caudate (Cau), and thalamus.

Table 1 | Demographic and neuropsychological data

	HC	PD		HC versus PD-OFF		PD-OFF versus PD-ON	
		PD-OFF	PD-ON	t-/chi-stats	p-value	t-/chi-stats	p-value
Sample size	37	27		N/A		N/A	
Age (year)	71 ± 5	70 ± 6		1.01	0.28	N/A	
Sex (F/M)	22F/15M	14F/13M		0.66	0.55	N/A	
Education (years)	16 ± 2	17 ± 2		-1.11	0.27	N/A	
Disease duration (year)	N/A	4.26 ± 3.59		N/A		N/A	
LEDD	N/A	550.72 ± 270.22		N/A		N/A	
GDS	1.02 ± 2.34	2.33 ± 1.69		-2.47	0.02	N/A	
MOCA	27.31 ± 2.18	26.78 ± 3.04		0.80	0.42	N/A	
Maximum Disp (mm)	1.82 ± 1.47	1.41 ± 0.82	1.44 ± 0.58	1.30	0.20	0.70	0.84
Maximum FD (mm)	0.77 ± 1.12	0.58 ± 0.44	0.51 ± 0.23	0.96	0.39	0.82	0.35
MDS-UPDRS III	N/A	36.37 ± 12.47	23.78 ± 11.58	N/A		7.76	3.15e ⁻⁸
SDMT oral	53.3 ± 9.13	49.54 ± 8.49	48.63 ± 9.03	1.66	0.10	0.61	0.55
SDM written	49.54 ± 11.1	45.19 ± 9.99	46.78 ± 11.9	1.59	0.12	-1.12	0.26
Sternberg LL ACC (%)	97 ± 3	98 ± 3	97 ± 4	-0.97	0.34	1.27	0.21
Sternberg HL ACC (%)	93 ± 4	95 ± 5	94 ± 5	-2.41	0.02	1.30	0.21
Sternberg DL ACC (%)	96 ± 6	95 ± 5	96 ± 5	0.37	0.72	-0.23	0.82
Sternberg LL RT (sec)	1.00 ± 0.24	1.01 ± 0.20	0.99 ± 0.23	-0.07	0.94	0.46	0.65
Sternberg HL RT (sec)	1.26 ± 0.24	1.25 ± 0.20	1.30 ± 0.30	0.18	0.86	-0.90	0.38
Sternberg DL RT (sec)	1.29 ± 0.26	1.29 ± 0.23	1.31 ± 0.35	-0.03	0.98	-0.53	0.59

Table shows the mean ± standard deviation for HC and PD groups. p -values of HC versus PD-OFF are derived from two-sample t -tests. p -values of the PD-OFF and PD-ON are derived from paired-sample t -tests.

HC healthy controls, PD-OFF Parkinson's disease, off medication, PD-ON Parkinson's disease, on medication, F female, M male, LEDD levodopa equivalent daily dosage (mg/day), GDS geriatric depression scale, Disp displacement, FD frame-wise displacement, MDS-UPDRS III movement disorders society-unified Parkinson's disease scale motor score, SDMT Oral symbol digit modalities test, oral adjusted T score, SDMT Written symbol digit modalities test, written adjusted T score, LL low load, HL high load, DL distractor load, ACC accuracy, RT reaction time.

specifically associated with stimulus encoding and State 4 is associated with maintaining and retrieving information. Notably, we observed load-dependent gradual increase of the posterior probability of State 4 during the maintenance and retrieval phases, suggesting that State 4 is modulated by cognitive load.

Interestingly, the BDS-derived state transition matrix further revealed that transition between State 1 and State 4 does not occur directly, but rather occurs by passing through State 2 and 3, respectively, in HL and DL conditions in all three groups (Fig. 3E and Supplementary Fig. 4). These results suggest that States 2 and 3,

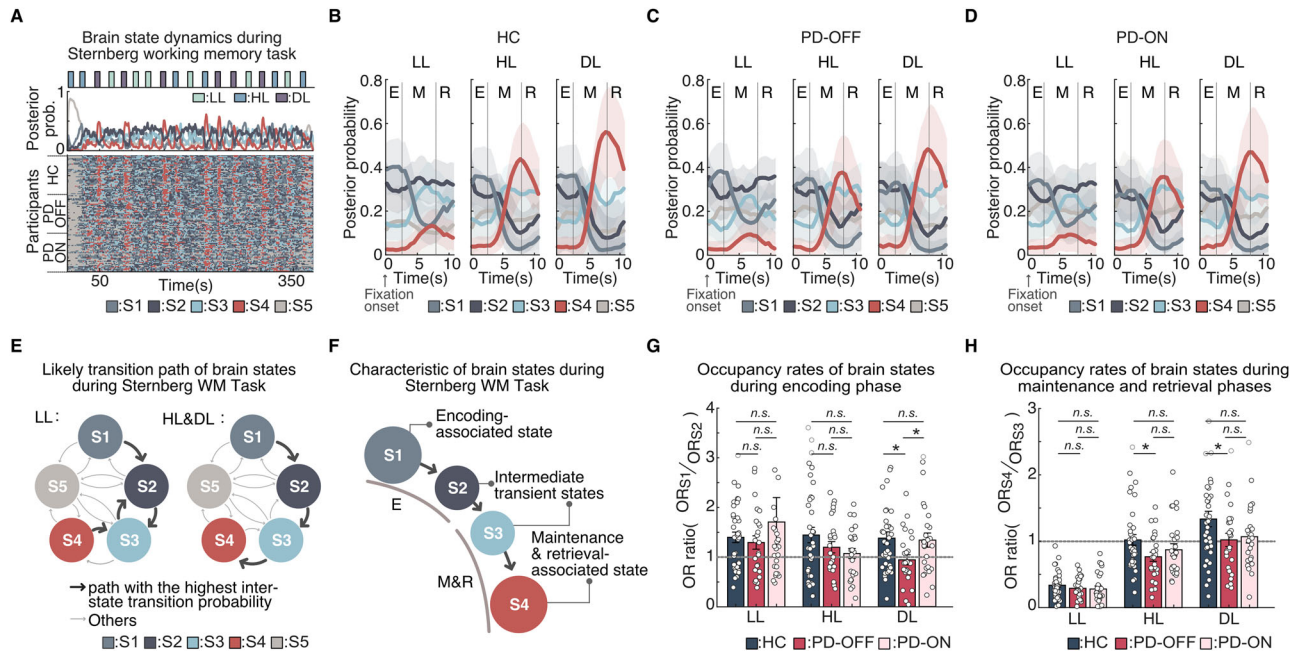


Fig. 3 | Dynamic temporal properties of brain states associated with the Sternberg working memory task. **A** The scan session comprised four task runs, each with six randomly intermixed low-load (LL), high-load (HL), and distractor-load (DL) trials. Task design of the three load conditions in run A (top). Averaged time-varying posterior probability of the five brain states across HC, PD-OFF, and PD-ON groups (middle). Temporal evolution of the brain states identified in each group (bottom). **B–D** Averaged time-varying posterior probabilities of brain state corresponding to *Fixation Onset* to 1 s after *Response Onset* for HC, PD-OFF, and PD-ON groups. Each task phase was separated by vertical dashed lines (E: Encoding, M: Maintenance, R: Retrieval). The posterior probability of each brain state showed distinct temporal profiles across different task phases. Data are presented as mean values \pm SEM. **E** The likely switching path of the brain states during the task performance. The most likely switching path across the three task phases is State 1 \rightarrow 2 \rightarrow 3 for LL condition, and State 1 \rightarrow 2 \rightarrow 3 \rightarrow 4 for HL and DL conditions. **F** Schematic

illustrating dynamic evolution of brain state dynamics during the task. **G** The occupancy rate of brain states during the encoding phase. The relative occupancy rate of State 1 over State 2 is significantly lower in PD-OFF group compared to HC and PD-ON groups in the DL condition. The horizontal line at $y=1$ represents the threshold where the dominance of State 1 exceeds that of its neighboring intermediate state, State 2. **H** The occupancy rate of brain states during the maintenance and retrieval phases. The relative occupancy rate of State 4 over State 3 is significantly lower in PD-OFF group compared to HC group in the HL and DL conditions. The horizontal line at $y=1$ represents the threshold where the dominance of State 4 exceeds that of its neighboring intermediate state, State 3. **G, H** Data are presented as mean values \pm SEM. * $p < 0.05$, n.s. $p \geq 0.05$. p -values were determined by two-tailed t -test, with FDR correction, $n_{HC} = 37$, $n_{PD} = 27$; all exact p -values are provided in Source Data. Source data are provided as a Source Data file.

respectively, serve as intermediary transient states facilitating the transition from State 1 to State 4, the dominant states associated with the memory encoding and maintenance-retrieval phases of the Sternberg working memory task (Fig. 3F).

Aberrant brain state dynamics in PD and its remediation by dopaminergic medication

We sought to determine whether brain state dynamics differ between PD and the HC group during the performance of the Sternberg working memory task. We compared the occupancy rate of brain states between all three groups (HC vs PD-OFF and PD-OFF vs PD-ON). The occupancy rate quantifies the proportion of time a particular state is selected as the dominant state. This measurement provides insight into how the brain’s temporal characteristics and states evolve to meet the varying demands of a dynamic task. Briefly, analysis of occupancy rates across task phases and conditions revealed that State 1 is the dominant brain state in encoding phase and State 4 is the dominant state in maintenance and retrieval phases (see Supplementary Result and Supplementary Fig. 5 for details). Analysis of load effects on occupancy rate revealed that the occupancy rate of State 4 was significantly higher in HL than LL and in DL than HL conditions for all groups (all $ps < 0.05$, paired two-tailed t -test, FDR-corrected, Supplementary Fig. 5D–F), demonstrating that State 4 is modulated by cognitive load and critical for maintaining and retrieving information.

First, we examined group differences in occupancy rate during the encoding phase. A two-way analysis of variance (ANOVA) with factors group (HC vs PD-OFF) and load condition (LL vs HL vs DL)

revealed a significant group effect such that PD-OFF had a lower occupancy rate of State 1 compared to HCs ($F_{1, 62} = 5.99$, $p = 0.02$, see Supplementary Table 2 and Supplementary Result for *post-hoc* analysis); no significant main effects or group \times load interactions were observed in the four other brain states ($ps > 0.05$). Similarly, during the maintenance and retrieval phases, there was a significant group effect such that PD-OFF had a lower occupancy rate of State 4 ($F_{1, 62} = 13.98$, $p = 0.0002$, see Supplementary Table 3 and Supplementary Result for *post-hoc* analysis) and there was no other significant group main effect in the four other brain states (all $ps > 0.05$, see Supplementary Table 3). When examining differences between PD-OFF and PD-ON with a similar two-way repeated ANOVA, we found a significant group effect such that PD-OFF had a higher occupancy rate of State 2 across all the task phases (all $ps < 0.05$, see Supplementary Tables 4, 5 and Supplementary Result for *post-hoc* analysis).

To test the hypothesis that PD patients have a reduced ability to maintain task-phase-specific states—State 1 during encoding and State 4 during maintenance/retrieval—we first assessed their engagement in these states. We then calculated the relative occupancy ratios of State 1 and State 4 compared to their neighboring intermediate states, State 2 and State 3, respectively (Fig. 3F). During the encoding phase, dominance of State 1 was significantly lower in PD-OFF compared to HC ($p = 0.029$, unpaired two-tailed t -test, Fig. 3G), and significantly lower in PD-OFF compared to PD-ON ($p = 0.023$, paired two-tailed t -test, Fig. 3G) in the DL condition. In maintenance and retrieval phases, dominance of State 4 was significantly lower in PD-OFF than HC in HL ($p = 0.026$, unpaired two-tailed t -test, Fig. 3H), and DL ($p = 0.049$,

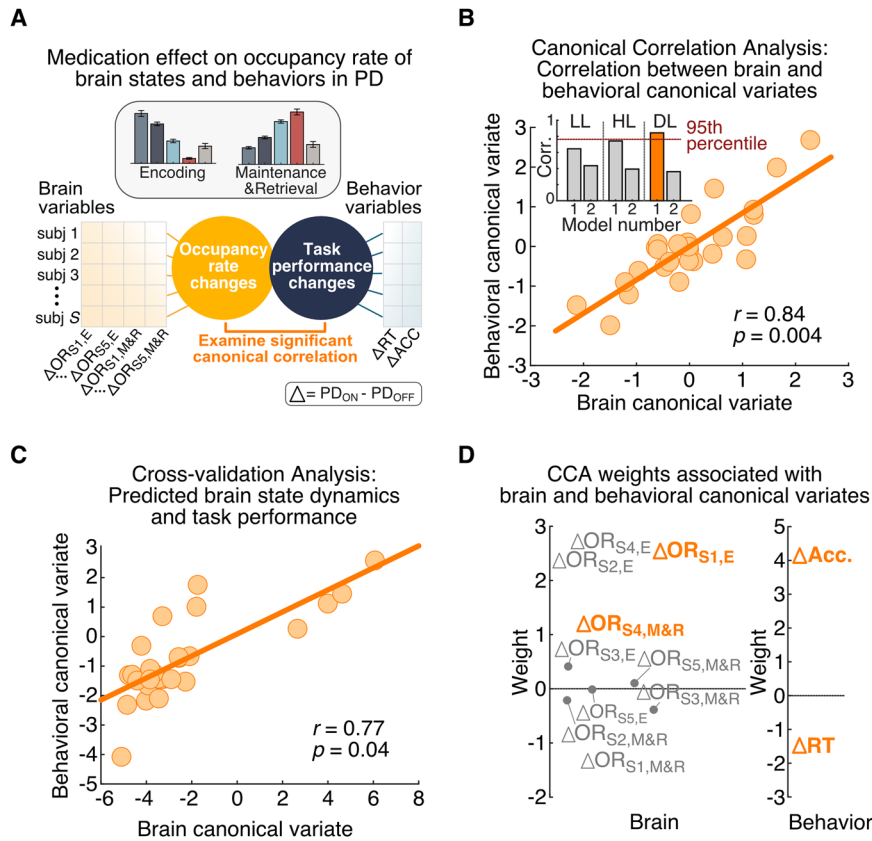


Fig. 4 | Medication effect on occupancy rate of brain states and task performance in the Parkinson's disease (PD) group. **A** In each load condition, we examined significant mode of covariation between dynamic brain measures of brain state (assessed using changes of phase-specific occupancy rates of brain states during (i) encoding phase and (ii) concatenated maintenance-and-retrieval phase), and task performance (assessed using changes in task performance including accuracy and reaction time). **B** Canonical correlations showing modes against the null distribution of the permuted canonical correlations estimated via permutation testing ($r = 0.84$, $p = 0.004$, permutation test, FDR-corrected, $n_{PD} = 27$). This analysis revealed a significant Canonical Correlation Analysis (CCA)

component that represents changes in occupancy rate related to changes in task performance in DL condition. **C** Prediction analysis performed using leave-one-out cross-validation revealed that, based on changes in phase-specific occupancy rates of brain states, our CCA model can predict changes in task performance of PD patients on unseen data ($r = 0.77$, $p = 0.04$, Pearson's Correlation, $n_{PD} = 27$). **D** CCA weights associated with each canonical variate are shown. Variables showing significant contribution to the CCA mode are marked in yellow ($p < 0.05$, FDR-corrected, Pearson's Correlation, see *Methods* for details). **B–D** Source data are provided as a Source Data file.

unpaired two-tailed *t*-test, Fig. 3H) conditions. No significant differences were observed between HC and PD-ON, and within PD groups in all load conditions (all $ps > 0.05$, two-tailed *t*-test, Fig. 3H). Notably, all major findings remain consistent when analyzing only the cognitively normal PD participants and excluding the 5 PD-MCI participants (Supplementary Fig. 6).

Taken together, these results demonstrate that brain state dynamics in PD are aberrant, revealing weaker engagement of phase-appropriate dominant states during distinct task stages. Notably, these results identified State 1 and State 4, the dominant states in the encoding and maintenance/retrieval, respectively, as being dysfunctional in PD-OFF. The aberrant brain-state dynamics were then remediated by dopaminergic medication in PD participants.

Dopaminergic medication effects on brain state dynamics and working memory task performance in PD

Next, we investigated whether individual variations in the effects of dopaminergic medication on brain state dynamics impacts task performance. We performed Canonical Correlation Analyses (CCA) to determine the relation between medication-induced changes in occupancy rate and task performance in each load condition. The input to the CCA consisted of load-specific brain variables (i.e., differences in occupancy rates of brain states during encoding and maintenance-retrieval between ON and OFF medication states) and

load-specific behavioral variables (i.e., differences in RT and accuracy between ON and OFF medication states) (Fig. 4A). Permutation testing revealed a significant CCA component linking changes in occupancy rate to changes in task performance in DL task condition (FDR-corrected, $p < 0.05$, Fig. 4B). Moreover, LOOCV further demonstrated that our CCA model could robustly predict dopamine-induced changes in task performance on unseen data (Fig. 4C). Importantly, occupancy rate alterations of State 1 during the encoding phase and State 4 during the maintenance and retrieval phases had positive weights within the brain component, while accuracy displayed a positive weight and RT had a negative weight in the behavioral component (FDR-corrected, $p < 0.05$, Fig. 4D). This pattern suggests that an increased occupancy rate of States 1 (encoding) and 4 (maintenance and retrieval) is associated with medication-induced improvements in task accuracy and faster RT (Fig. 4D).

These results underscore that dopaminergic medication ameliorates the specific dysfunction in States 1 and 4 in PD, the dominant states responsible for encoding and maintenance/retrieval, respectively.

Dopaminergic medication effects on state-specific functional connectivity patterns in PD

The identification of brain States 1 and 4 as significantly impacted in PD patients led us to a focused inquiry into how medication changes

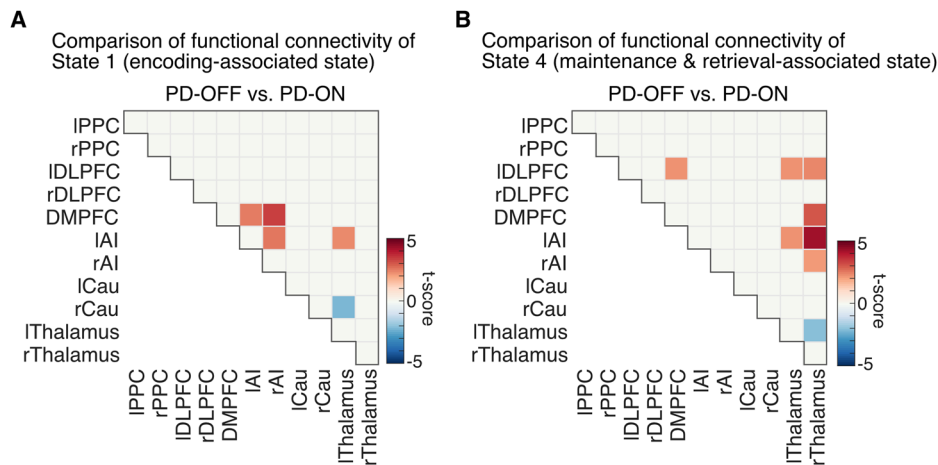


Fig. 5 | Dopaminergic medication effects on state-specific functional connectivity patterns in Parkinson's disease (PD) group. A BSDS identified differences in functional connectivity patterns of the encoding-associated brain state (i.e., S1) between PD-OFF and PD-ON groups. Compared to PD-ON, PD-OFF had significantly increased functional connectivity between DMPFC and bilateral AI. Also, right Thalamus showed increased functional connectivity with left AI and decreased functional connectivity with right Caudate, respectively ($p < 0.05$, two-tailed t -test, FDR corrected, $n_{PD} = 27$). **B** BSDS also identified difference in functional connectivity patterns of the maintenance-retrieval-associated brain state

(i.e., S4) between PD-OFF and PD-ON groups. Compared to PD-ON, PD-OFF had significantly increased functional connectivity of Thalamus with DLPFC, DMPFC, and AI, and had significantly reduced functional connectivity between left and right Thalamus ($p < 0.05$, two-tailed t -test, FDR corrected, $n_{PD} = 27$). **A, B** The ROIs include bilateral posterior parietal cortex (PPC), dorsolateral prefrontal cortex (DLPFC), dorsomedial prefrontal cortex (DMPFC), anterior insula (AI), caudate (Cau), and thalamus. All exact p -values are provided in Source Data. Source data are provided as a Source Data file.

state-specific functional connectivity patterns. We leveraged BSDS which provides state-specific measures of inter-regional functional connectivity. During memory encoding, compared to PD-ON, PD-OFF showed significantly increased functional connectivity between bilateral AI and DMPFC, and between left AI and left Thalamus in State 1 ($p < 0.05$, FDR-corrected, Fig. 5A and Supplementary Fig. 7). The left thalamus also showed decreased functional connectivity with right Caudate ($p < 0.05$, FDR-corrected, Fig. 5A and Supplementary Fig. 7) in PD-OFF. During memory maintenance and retrieval, compared to PD-ON, PD-OFF showed significantly increased functional connectivity of Thalamus with DLPFC, DMPFC, and AI, and significantly decreased functional connectivity between left and right Thalamus in State 4 ($p < 0.05$, FDR-corrected, Fig. 5B and Supplementary Fig. 7).

Dopaminergic medication effects on functional connectivity and working memory task performance

Next, we investigated individual variations in the effect of dopaminergic medication on changes in functional connectivity patterns and task performance. We performed CCA to determine the relationship between medication effects on functional connectivity and task performance for each load condition. Input to the CCA consisted of brain variables: connectivity strength changes of the links that significantly differentiated PD-OFF and PD-ON conditions in State 1 and State 4 (Fig. 5); and load-specific behavioral variables: changes in RT and accuracy between PD-ON and PD-OFF (Fig. 6A). Permutation testing revealed a significant CCA component that captured significant medication-induced changes in functional connectivity and task performance in the demanding DL condition (FDR-corrected, $p < 0.05$, Fig. 6B). Moreover, LOOCV further demonstrated that our CCA model could predict dopamine-induced changes in task performance on unseen data (Fig. 6C). Increased bilateral thalamus connectivity of State 4 and decreased left DLPFC-left thalamus connectivity of State 4 were associated with increased accuracy in the DL condition (FDR-corrected, $p < 0.05$, Fig. 6D). These results demonstrate that changes in dynamic functional connectivity contributes to individual changes in working memory task performance in PD.

Medication dosage effects on brain state dynamics and task performance in PD

Finally, we determined an association between dopaminergic medication dosage, spatiotemporal brain state dynamics, and task performance in PD. Changes in temporal and spatial brain state dynamics and task performance were assessed by brain canonical variate and behavioral canonical variate from significant CCA modes identified in Fig. 4B and Fig. 6B, respectively. Interestingly, this analysis revealed that dopaminergic medication dosage has an inverted-U-shaped relationship with brain ($r^2 = 0.33$, Fig. 7A and Supplementary Fig. 8A) and behavioral ($r^2 = 0.20$, Fig. 7B and Supplementary Fig. 8B) canonical variates that we identified in Fig. 4B, suggesting that medication dosage impacts temporal brain state dynamics and task performance in PD. In contrast, dopaminergic medication dosage was not significantly associated with brain and behavioral measures identified in Fig. 6 (Supplementary Fig. 9). These results demonstrate that the ability to engage and sustain task-phase-specific brain states is closely linked to the dosage of dopaminergic medication. Specifically, we identified a nonlinear relationship between medication dosage, brain state dynamics, and task performance. Optimal dosage, which aligns with appropriate brain state dynamics is associated with enhanced task performance. In contrast, both insufficient and excessive dosages are linked to suboptimal brain state engagement and diminished task performance.

Discussion

We employed Bayesian state-space modeling to probe how dopaminergic medication impacts dynamic neural circuits during working memory tasks in PD participants, and how these changes are connected to individual variations in cognitive performance changes induced by dopaminergic medication. A within-subject approach, in which we tracked working memory performance during fMRI scanning in both medicated and unmedicated states, allowed us to thoroughly assess the effects of dopaminergic medication on brain state dynamics and task performance. Our data analysis revealed two primary brain states associated with distinct phases of the working memory task. These states were activated in both healthy individuals and PD participants, regardless of medication status. However, the dominance of

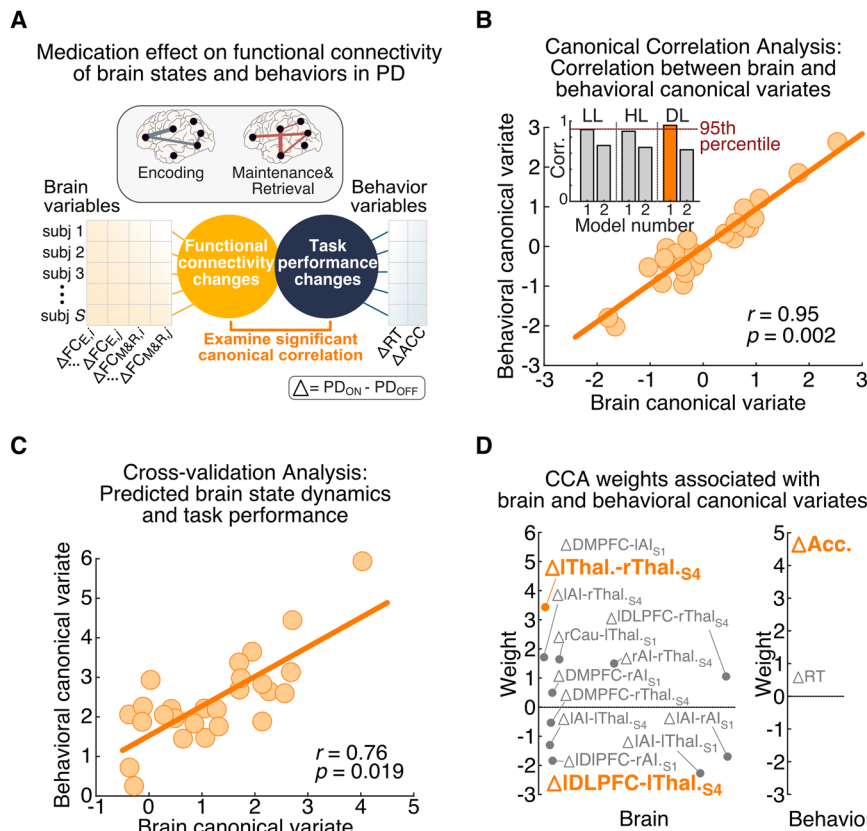


Fig. 6 | Medication effect on functional connectivity pattern of brain states and task performance in the Parkinson's disease (PD) group. **A** Medication effect on functional connectivity brain states and task performance in PD. We examined significant modes of covariation between dynamic brain measures of brain state (assessed using changes of functional connectivity in encoding-associated and maintenance-retrieval-associated brain states), and task performance (assessed using changes in task performance including accuracy and reaction time). **B** Canonical correlations showing modes against the null distribution of the permuted canonical correlations estimated via permutation testing ($r = 0.95$, $p < 0.05$, permutation test, FDR-corrected, $n_{PD} = 27$). This analysis revealed a significant

Canonical Correlation Analysis (CCA) component that represents significant medication-related changes in functional connectivity and task performance in DL condition. **C** Prediction analysis performed using leave-one-out cross-validation revealed that, based on changes in functional connectivity pattern in State 1 and State 4, our CCA model can predict changes in task performance of PD patients on unseen data ($r = 0.76$, $p = 0.019$, Pearson's Correlation, $n_{PD} = 27$). **D** CCA weights associated with each canonical variate are shown. Variables showing significant contribution to the CCA mode are marked in yellow ($p < 0.05$, FDR-corrected, Pearson's Correlation, $n_{PD} = 27$, see *Methods* for details). **B–D** Source data are provided as a Source Data file.

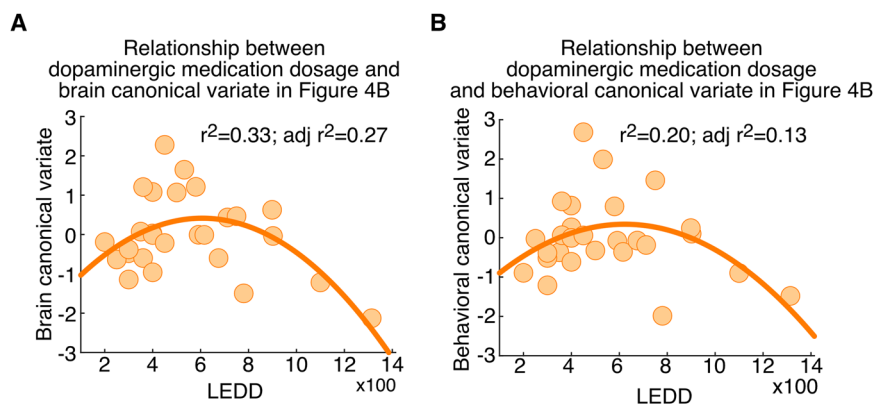


Fig. 7 | Medication dosage effects on brain state dynamics and task performance in the Parkinson's disease (PD) group. **A** Relationship between dosage of dopaminergic medication and brain canonical variate ($n_{PD} = 27$). **B** Relationship

between dosage of dopaminergic medication and behavioral canonical variate ($n_{PD} = 27$). LEDD = Levodopa equivalent daily dosage (mg/day).

these states was significantly reduced in PD participants, particularly during more challenging conditions when they were off medication. Notably, increased engagement of specific brain states during medicated periods correlated with improved task performance in PD

patients. Additionally, we uncovered a non-linear inverted-U relationship between the dosage of dopaminergic medication, brain state dynamics, and task performance. Our findings offer valuable insights into dynamic mechanisms influencing individual differences in

treatment response and suggest potential avenues for personalizing treatment strategies in PD.

The first objective of our study was to probe the dynamics of brain states associated with Sternberg working memory task performance in PD participants and to assess the influence of dopaminergic medication on these dynamics. In a prior study, we utilized BSDS to determine optimal brain states during the Sternberg task in HCs and showed strong correlation between these brain state dynamics and task performance²⁷. In the current study, we extended the findings by employing the BSDS model, initially trained in HCs, to fit fMRI data in PD participants. This model-based approach enabled us to analyze the deviation of brain state dynamics in PD patients from those in HCs. Moreover, it provided us with a valuable framework to investigate the impact of dopaminergic medication on these brain states in individuals with PD.

Optimal cognitive functioning is largely predicated on dynamic and flexible reconfiguration of brain states that transiently link distributed brain regions^{26,27,32–35}. Prior research using resting-state fMRI points to aberrant functional connectivity in PD^{44–48}, and there is also evidence for altered temporal dynamics of functional connectivity in the resting state in PD^{47,48}. However, resting-state fMRI offers limited insights into the mechanisms driving brain activity during cognition as dynamics change with task context.

Untangling brain states associated with the distinct components of working memory, such as encoding, maintenance and retrieval, has been challenging because most fMRI scans have poor temporal resolution in comparison to trial duration. Using ultra-fast task fMRI data with a temporal resolution of 0.49 s to overcome this challenge; this fast sampling allowed us to uncover context-dependent dynamic processes that are typically not observable with conventional approaches. State space modeling identified two dominant brain states associated with distinct phases of the working memory task. Both HC and PD participants—whether ON or OFF dopaminergic medication—engaged Brain State 1 during encoding, and Brain State 4 during the maintenance and retrieval phases of the task. However, PD participants showed a marked reduction in the dominance of these states, especially during the more challenging task trials when participants were OFF dopaminergic medication. These results demonstrate that the temporal dynamics of brain states that occur during distinct phases of working memory is aberrant in PD.

Our second objective was to elucidate neural dynamic mechanisms underlying individual variations in the effect of dopaminergic medication on task performance. Dopaminergic medications like levodopa and other dopaminergic agonists are effective in alleviating PD's motor symptoms⁴⁹. However, their impact on cognition in PD varies considerably across individuals and is likely influenced by person-specific factors such as differences in medication history, dosage, type of medication used, metabolism, and dopamine regulation^{49,50}. Given the wide range of factors that can influence dopaminergic medication-related cognitive changes, examination of within-subject changes has the potential to provide better insight into mechanisms of treatment response.

We leveraged the within-subject design in PD participants to determine whether medication-induced changes in brain states are related to changes in task performance when PD participants were medicated compared to when they were unmedicated. We examined this relationship across the three task load conditions using Canonical Correlation Analysis (CCA). Our analysis revealed a significant relationship between medication-induced changes in occupancy rate of dynamic brain states and medication-induced changes in task performance in the distractor-load (DL) condition (Fig. 4B), which requires both the maintenance in memory of task-relevant stimuli and suppression of irrelevant distractors. Cross-validation analysis further validated the robustness of our findings, confirming that its ability to accurately predict brain-behavior relationships associated with

medication-induced changes in unseen data. Importantly, higher occupancy rates of State 1 and 4—associated with stimulus encoding and maintaining/retrieving information, respectively—in the DL condition, were linked to higher task accuracy and faster RT when PD participants were medicated compared to when they were unmedicated.

These results suggest that dopamine-induced enhancement of task-specific brain states contributes to improved behavioral performance, offering valuable insights into the neural mechanisms by which dopaminergic medication enhances or impairs cognitive functions in PD participants.

Our third objective was to determine the effect of dopaminergic medication on brain circuits and identify the mechanisms by which they impact task performance in PD. In advance over previous studies, our state-space modeling identified dynamic brain connectivity associated with specific phases of working memory. Previous studies in PD patients have reported abnormal activity and disrupted functional connectivity during working memory in PD in comparison to HCs^{28–31} but the state-dependent effects of dopaminergic medication in PD are poorly understood.

We focused our analysis on brain States 1 and 4, which were found to be dysfunctional in PD. Importantly, these states dominate the encoding, maintenance, and retrieval phases of the Sternberg working memory task. In the encoding phase, dopaminergic medication reduced functional connectivity of the anterior insula (AI) with the DMPFC and thalamus, and between the left and right AI in State 1. In contrast, dopaminergic medication decreased functional connectivity between thalamus and caudate. In the maintenance and retrieval phase, dopaminergic medication reduced functional connectivity of the thalamus with the AI, DMPFC, and DLPFC. In contrast, dopaminergic medication increased functional connectivity between left and right thalamus. These results suggest that the predominant effect of dopaminergic medication in PD is to reduce cortical hyperconnectivity in the encoding phase and thalamus-cortical circuits in the maintenance and retrieval phase. Our findings thus demonstrate that medication-induced changes in functional connectivity depend on task phase, likely reflecting the dynamic role of dopamine in cognitive functioning¹⁵.

Importantly, medication-induced changes in the patterns of functional connectivity were associated with changes in task performance. Specifically, CCA revealed that increased bilateral thalamic functional connectivity and decreased connectivity between left thalamus and left DLPFC during the maintenance and retrieval phase was associated with increased task accuracy in more complex DL task condition (Fig. 6D). These results demonstrate that alteration of thalamus-cortical functional connectivity in response to dopaminergic medication is associated with improved working memory task performance in PD patients (Fig. 6D).

Our findings suggest that dopaminergic modulation of cortical-subcortical functional connectivity, leading to improvements in working memory task performance in PD. This insight not only aligns with existing evidence of abnormal frontoparietal-basal ganglia circuit functioning in PD, but also sheds light on the dynamic nature of these alterations and their direct relevance to cognitive performance.

Our final objective was to identify an association between dopaminergic medication dosage and brain state dynamics during working memory. Interestingly, we found an inverted-U-shaped relationship between dopaminergic medication dosage, brain state dynamics, and task performance (Fig. 7). A wealth of literature has demonstrated an inverted U-shaped relationship between dopamine and working memory such that low and high prefrontal dopamine are associated with reduced working memory performance^{51–53}. This literature converges with our results showing that medication dosage had an inverted U-shape relationship with the brain canonical variate constructed by a combination of occupancy rate ($r^2 = 0.33$, Fig. 7A) and an

inverted U-shape relationship with the corresponding behavioral canonical variate ($r^2 = 0.20$, Fig. 7B) in the DL condition. Although our results cannot point to directionality, it is possible that low and high dopaminergic medication dosage leads to suboptimal engagement of encoding and maintenance/retrieval brain states, which then leads to reduced working memory performance.

Our finding of an inverted-U shaped relationship aligns with a model proposed by Cools and D'Esposito¹². In their study of healthy controls, they suggested that dopamine's effects on cognitive function follow an inverted-U profile, where both insufficient and excessive dopamine leads to suboptimal cognitive performance. This model suggests that there is an optimal level of dopamine for working memory processes, and deviations from this optimum, in either direction, is associated with poorer performance. It is important to consider, however, that the optimal level of dopamine for working memory processes may be different than the optimal level of dopamine for other cognitive processes and for motor functioning. Clinically, it is important to note that the optimal dose may vary depending on the target symptom. Our results lend empirical support to this model in the context of PD. We observed that individual differences in the dosage of dopaminergic medication and the resulting alterations in brain state dynamics corresponded to changes in cognitive performance. Specifically, an optimal dosage (associated with optimal brain state dynamics) was associated with improved task performance, whereas both lower and higher dosages were linked to poorer performance. This extends the inverted-U model by demonstrating its applicability to real-world clinical scenarios involving medication management in PD, and emphasizes the importance of fine-tuning dopaminergic therapy for optimal cognitive outcomes.

Critically, our findings uncover a nonlinear relationship between medication dosage and both brain state dynamics and task performance, illuminating a complex interaction that may guide future precision dosing strategies in the treatment of PD.

While our study offers valuable insights into the dynamic neural mechanisms underlying individual differences in dopaminergic treatment response in PD patients, several limitations warrant consideration, providing opportunities for future research. First, we used automatic Relevance Determination priors for high-dimensional variable selection, driven by prior validation and computational efficiency²⁶, as well as their common use in the modern machine learning^{54–56}. However, the selection of priors and inference in Bayesian modeling remains an area of ongoing debate in the field. Future work should explore alternative priors and modeling approaches to enhance robustness^{56,57}. Second, while our methodology has been rigorously validated in prior studies, including simulations and optogenetic stimulation²⁶, the neuroscience community has not yet reached consensus on the most suitable biophysically realistic models for validating methods for validating brain state dynamics. Future investigations should compare state-space models like ours against a wider array of biophysically realistic simulations, extending beyond those covered in our previous work²⁶. Third, although we used dopaminergic medication dosage to explore the relationship between dopamine and brain dynamics, we lack precise data on the extent of dopamine depletion in each participant before starting dopaminergic treatment. Relatedly, there may be individual differences in the absorption rate of dopaminergic medications. While LEDD provides an estimate of the total daily dopaminergic medication, it cannot disentangle the effects of different dopamine agonists which have different mechanisms of action. Finally, clinically, it is important to recognize that the optimal dopamine level for working memory may differ from the levels needed for other cognitive functions or motor control.

In summary, we employed innovative computational methods to probe the influence of dopamine on the brain state dynamics that underlie the encoding, maintenance, and retrieval subprocesses of working memory. This analysis allowed us to delve deeper into the

dynamic circuit processes involved in specific phases of working memory processing in individuals with PD. We discovered that changes induced by dopamine in the dynamic spatiotemporal properties of brain state dynamics correlated with individual differences in task performance gains among PD participants. This relation demonstrates a link between the brain's dynamic state and the observable changes in cognitive performance in individuals with PD. Critically, our findings offer valuable insights into medication-induced remediation of abnormal brain state dynamics and circuitry that occur during working memory processes in PD. Our results underscore the value of studying brain dynamics from an individual difference perspective and highlights the interplay between dopamine, brain dynamics, and working memory performance in PD. Our study demonstrates the potential of state-space computational methods in unraveling brain circuit dysfunction and its remediation in PD. This understanding could pave the way for more targeted therapeutic strategies and personalized treatments in the future, ultimately enhancing the quality of life for individuals with PD.

Methods

Participants

All participants were enrolled in the Alzheimer's Disease Research Center at the Stanford University School of Medicine. Inclusion criteria for healthy controls (HC) included age >60 years and cognitively unimpaired as determined by clinical consensus based on a neurological examination, functional assessment, and formal neuropsychological assessment that included National Alzheimer's Coordinating Center Uniform Data Set (version 3) tests. Individuals were excluded if a major psychiatric disorder was the primary cause of parkinsonism in PD participants, or if a psychiatric disorder was likely to affect cognition or motor functioning if they were a HC. Mean + SD geriatric depression scale-15 item (GDS-15) score⁵⁸ were 1.02 ± 2.34 for HC and 2.33 ± 1.69 for PD participants, indicating that the overall depression severity in this cohort was low (Supplementary Fig. 1). PD was determined by UK Brain Bank criteria⁵⁹ after a comprehensive neurological screening examination that included the Movement Disorders Society-Unified Parkinson's disease Rating Scale motor assessment (MDS-UPDRS part III)⁶⁰ both OFF and ON dopaminergic medications. PD participants also completed functional assessment and formal neuropsychological testing consistent with the National Alzheimer's Coordinating Center (26 PD cognitively unimpaired and 7 PD with mild cognitive impairment). Neuropsychological testing occurred within 6 months of the fMRI session. A total of 48 HC completed the Sternberg task in one fMRI session and 37 PD participants completed a modified Sternberg task²⁶ in two separate ON and OFF fMRI sessions. Two participants (2 HC) were excluded for excessive motion (i.e., mean motion >1.5 standard deviations above the interquartile range) and seven participants (3 HC, 4 PD) were excluded due to failure to complete all 4 task runs during the scan. Additionally, to investigate brain state dynamics during adequate task engagement, we selected subjects who correctly responded to 19 out of 24 trials, corresponding to $p < 0.01$ of success according to a binomial distribution in LL, HL, and DL condition (Fig. S1). Consequently, 37 HC (71 ± 5 years old; 22F/15M) and 27 PD participants (70 ± 6 years old; 14F/13M; 22 PD cognitively unimpaired and 5 PD with mild cognitive impairment) were included in the final analyses (see Table 1). All participants provided written consent and the Stanford University Institutional Review Board approved all study protocols.

Medication ON versus OFF order

To minimize the physical discomfort experienced by PD participants when are OFF dopaminergic medications, the OFF session was scheduled at a time based on patient convenience and preference; therefore, the ON versus OFF order was not fully counterbalanced across PD participants. The mean (SD) time between ON and OFF scan

was 17 (82) days with 10 PD participants who had their OFF scan first and 17 PD participants who had their ON scan first.

Sternberg task

The modified fMRI Sternberg working memory task³⁶, consisting of low-load (LL), high-load (HL), or distractor-load (DL) working memory conditions, assesses the ability to hold and manipulate information for a short period of time^{21–23}. Each PD participant completed the task in both ON and OFF medication sessions in a within-subject design. Each trial began with fixation (0.5 s) followed by an encoding phase (2 s) during which a set of stimuli was simultaneously displayed. The set of stimuli consisted of 5 identical numbers (LL condition), 5 different numbers (HL condition), or 5 different numbers along with 5 different characters (DL condition). The trial was then followed by a maintenance phase (6 ± 2 s), during which a fixed marker was displayed, and the presentation of a probe for 0.5 s. Participants indicated whether the probe matched any of the numbers displayed during the encoding phase. Accuracy and reaction time (RT) were recorded for each trial. Each scan included 4 task runs, which each consisted of 6 LL, 6 HL, and 6 DL working memory trials randomly intermixed. The stimulus presentations were implemented using E-Prime software (v2.0; Psychology Software Tools, Pittsburgh, PA; 2002) and projected at the center of the screen using a magnet-compatible projection system. Prior to each fMRI session, participants were trained with instructions and completed a practice session of the task.

fMRI acquisition and preprocessing

The fMRI images were collected using a 3T scanner. A total of 790 functional images were acquired using multiband echo-planar imaging with the following parameters: 42 slices, repetition time (TR) = 490 ms, flip angle 45°, echo time = 30 ms, field of view = 220 × 220 mm, matrix = 74 × 74, 3 mm slice thickness, and voxel size = 2.97 × 2.97 × 3 mm. The first 12 time points were removed to allow for signal equilibration, leaving 778 time points for each subject. Each subject's T1-weighted anatomical scan had been acquired using a magnetization-prepared rapid-acquisition gradient echo (MPRAGE) sequence (256 slices with a 176 × 256 matrix; voxel size 1.00 × 0.977 × 0.977 mm³). All fMRI data were preprocessed using SPM12, as well as in-house programs in MATLAB (MathWorks). fMRI data were first slice time corrected, aligned to the averaged time frame to correct for head motion, and co-registered with each participant's T1-weighted images. Structural MRI images were segmented into grey matter, white matter, and cerebrospinal fluid. Based on the transformation matrix from structural image, the functional images were then transformed to the standard Montreal Neurological Institute (MNI) template in 2 × 2 × 2 mm³ by using the Diffeomorphic Anatomical Registration Through Exponentiated Lie algebra (DARTEL, Ashburner et al. 2007) toolbox. A 6-mm Gaussian kernel was used to spatially smooth the functional images. Subjects with more than 3 mm head motions were excluded.

Working memory network

To define the ROIs, we examined whole-brain activation patterns associated with the Sternberg DL vs. LL and HL vs. LL contrasts in HCs. Consistent with previous studies^{22–25}, the Sternberg task strongly activated the frontal-parietal system, as well as the thalamus and caudate. The Brainnetome atlas⁶¹ was used to demarcate ROIs in: (1) left posterior parietal cortex (lPPC), (2) right posterior parietal cortex (rPPC), (3) left dorsolateral prefrontal cortex (lDLPFC), (4) right dorsolateral prefrontal cortex (rDLPFC), (5) bilateral DMPFC, (6) left anterior insula (lAI), (7) right anterior insula (rAI), (8) left caudate (lCau), (9) right caudate (rCau), (10) left thalamus (lthalamus), (11) right thalamus (rthalamus). The time series of each ROI was calculated by taking the average of the time series of all voxels within each ROI. A multiple linear regression approach with 6 realignment parameters

(3 translations and 3 rotations) was applied to account for head motion-related artifacts and the resulting time series were further linearly detrended, normalized, and high-pass filtered (>0.008 Hz).

Bayesian switching dynamical system model

We used a BSDS model²⁶ to investigate brain state dynamics underlying the Sternberg working memory task in HC and PD groups. We used a variational Bayesian (VB) framework^{62,63} to infer model parameters, including the number of brain states. The number of states is treated as a random variable, whose optimal value is learned from data using automatic relevance determination procedures implemented in a VB framework (Supplementary Fig. 2).

We previously used BSDS (BSDS) model in HC group and showed that optimal task performance requires engagement of brain states in a timely manner²⁷. In this study, we used the BSDS model trained on the HC data to fit the PD data. This allowed us to use brain states in HCs as the reference, examine how brain state dynamics in PD participants deviate from HCs, and determine how dopaminergic medication impacts brain state dynamics in PD. BSDS was initialized with 10 states and it converged to 5 states. Detailed methods can be found in Supplementary Methods.

Temporal properties of brain states

BSDS estimated the posterior probability of each brain state at each time point and chose the brain state with highest probability as the dominant state at that time point. Using the temporal evolution of the brain states, we measured temporal properties of each brain state in each task condition (LL, HL, and DL), including occupancy rate and state switching probability. Occupancy rate quantifies the proportion of time that a state is chosen as the dominant state. State switching probability quantifies the chance that brain state at time point t either remains at its own state or switch to another brain state at the time point $t + 1$. These temporal properties were examined to characterize each task condition and further used to examine their relationship with medication-induced cognitive changes (PD-ON vs PD-OFF).

Dynamic functional connections that distinguish HC and PD groups

To identify dynamic functional connections that distinguish groups, we converted covariance matrices derived from the BSDS model to Fisher's-transformed-Pearson's correlation matrices per brain state per subject. The resulting correlation values were then z-transformed, representing subject-state-wise functional connection strength. Group differences between HC and PD-OFF were examined using unpaired two-tailed t -tests. The effects of dopaminergic medication in PD were examined using paired two-tailed t -tests comparing PD-OFF and PD-ON. All tests were corrected for multiple comparisons using FDR correction at $p < 0.05$.

Medication effects on the relationship between brain state dynamics and task performance in PD

CCA^{64,65} was used to determine the dopaminergic medication effects on relationship between two distinct spatiotemporal properties of brain states and Sternberg working memory task performance in the PD group. In first analysis, separate CCAs were conducted for each load condition to examine the relationship between medication-induced alterations in occupancy rates of brain states and medication-induced alterations in task performance (i.e., accuracy and RT). In second analysis, separate CCAs were conducted for each load condition to examine the relationship between medication-induced alterations in functional connectivity strength in each state and medication-induced alterations in task performance (i.e., accuracy and RT).

In each analysis, we estimated CCA modes (components) that maximized the correlation between brain state dynamics and behavioral performance scores. Sex, education level, and medication order

were regressed out from all brain and behavioral measures included in the analysis. For each CCA mode, permutation testing was used to test the significance of the corresponding canonical correlation. CCA was rerun after each permutation, and the canonical correlation was recalculated. These procedures were repeated 1000 times to build a null distribution of canonical correlations for comparison with the original canonical correlation. The p -values of each CCA dimension were corrected for multiple testing across the estimated CCA modes (FDR-corrected, $p < 0.05$). To infer the contribution of the original variables to the corresponding CCA models, we computed *Pearson's* correlation between each original brain variable and corresponding canonical variate, as well as *Pearson's* correlation between each original behavioral variable and corresponding canonical variate. The significant threshold was set at $p < 0.05$ with FDR correction. Next, prediction analysis was performed using leave-one-out-cross-validation (LOOCV). *Pearson's* correlation was used to evaluate the correlation between the predicted brain and cognitive variables. The statistical significance of the correlation was evaluated using permutation times (1000 times).

Relation between brain state dynamics and dopaminergic medication dosage

We investigated the association between dopaminergic medication dosage, changes in spatiotemporal brain state dynamics, and task performance within the PD group. To achieve this, we assessed changes in temporal and spatial brain state dynamics, as well as task performance, using brain canonical variates and behavioral canonical variates derived from a significant CCA mode identified through the procedure described in the section above. We examined their linear and nonlinear relationship with dopaminergic medication dosage using first- and second-order polynomial coefficients determined with MATLAB “polyfit” function.

Reporting summary

Further information on research design is available in the Nature Portfolio Reporting Summary linked to this article.

Data availability

All original data reported in this study are publicly available on Zenodo: <https://doi.org/10.5281/zenodo.14567445>⁶⁶. Source data are provided with this paper.

Code availability

The code used to perform the analyses in this study are publicly available on Zenodo: <https://doi.org/10.5281/zenodo.14567445>⁶⁶.

References

- Aarsland, D. et al. Parkinson disease-associated cognitive impairment. *Nat. Rev. Dis. Prim.* **7**, 47 (2021).
- Lang, A. E. & Lozano, A. M. Parkinson's disease. *N. Engl. J. Med.* **339**, 1130–1143 (1998).
- Moustafa, A. A. et al. Motor symptoms in Parkinson's disease: a unified framework. *Neurosci. Biobehav. Rev.* **68**, 727–740 (2016).
- Xia, R. & Mao, Z.-H. Progression of motor symptoms in Parkinson's disease. *Neurosci. Bull.* **28**, 39–48 (2012).
- Poewe, W. Non-motor symptoms in Parkinson's disease. *Eur. J. Neurol.* **15**, 14–20 (2008).
- Singh, N., Pillay, V. & Choonara, Y. E. Advances in the treatment of Parkinson's disease. *Prog. Neurobiol.* **81**, 29–44 (2007).
- Cools, R., Miyakawa, A., Sheridan, M. & D'Esposito, M. Enhanced frontal function in Parkinson's disease. *Brain* **133**, 225–233 (2010).
- Moustafa, A. A., Sherman, S. J. & Frank, M. J. A dopaminergic basis for working memory, learning and attentional shifting in Parkinsonism. *Neuropsychologia* **46**, 3144–3156 (2008).
- Skeel, R. L. et al. Basal ganglia dysfunction, working memory, and sentence comprehension in patients with Parkinson's disease. *Neuropsychologia* **39**, 962–971 (2001).
- Scherman, D. et al. Striatal dopamine deficiency in parkinson's disease: Role of aging. *Ann. Neurol.* **26**, 551–557 (1989).
- Bell, P. T. et al. Dopaminergic basis for impairments in functional connectivity across subdivisions of the striatum in Parkinson's disease. *Hum. Brain Mapp.* **36**, 1278–1291 (2015).
- Cools, R. & D'Esposito, M. Inverted-U-shaped dopamine actions on human working memory and cognitive control. *Biol. Psychiatry* **69**, e113–e125 (2011).
- Hazy, T. E., Frank, M. J. & O'reilly, R. C. Towards an executive without a homunculus: computational models of the prefrontal cortex/basal ganglia system. *Philos. Trans. R. Soc. B Biol. Sci.* **362**, 1601–1613 (2007).
- Landau, S. M., Lal, R., O'Neil, J. P., Baker, S. & Jagust, W. J. Striatal dopamine and working memory. *Cereb. Cortex* **19**, 445–454 (2009).
- Cools, R., Froböse, M., Aarts, E. & Hofmans, L. Dopamine and the motivation of cognitive control. *Handb. Clin. Neurol.* **163**, 123–143 (2019).
- Carceles-Cordon, M., Weintraub, D. & Chen-Plotkin, A. S. Cognitive heterogeneity in Parkinson's disease: a mechanistic view. *Neuron* **111**, 1531–1546 (2023).
- Cai, W. et al. Dopaminergic medication normalizes aberrant cognitive control circuit signalling in Parkinson's disease. *Brain* **145**, 4042–4055 (2022).
- Aarsland, D. et al. Mild cognitive impairment in Parkinson disease: a multicenter pooled analysis. *Neurology* **75**, 1062–1069 (2010).
- Watson, G. S. & Leverenz, J. B. Profile of cognitive impairment in Parkinson's disease. *Brain Pathol.* **20**, 640–645 (2010).
- Weintraub, D. et al. Cognitive performance and neuropsychiatric symptoms in early, untreated Parkinson's disease. *Mov. Disord.* **30**, 919–927 (2015).
- Baddeley, A. Working memory. *Science* **255**, 556–559 (1992).
- D'Esposito, M. & Postle, B. R. The cognitive neuroscience of working memory. *Annu. Rev. Psychol.* **66**, 115–142 (2015).
- Goldman-Rakic, P. S. Cellular basis of working memory. *Neuron* **14**, 477–485 (1995).
- Chang, C., Crottaz-Herbette, S. & Menon, V. Temporal dynamics of basal ganglia response and connectivity during verbal working memory. *NeuroImage* **34**, 1253–1269 (2007).
- Myers, N. E., Stokes, M. G. & Nobre, A. C. Prioritizing information during working memory: beyond sustained internal attention. *Trends Cogn. Sci.* **21**, 449–461 (2017).
- Taghia, J. et al. Uncovering hidden brain state dynamics that regulate performance and decision-making during cognition. *Nat. Commun.* **9**, 2505 (2018).
- Lee, B. et al. Latent brain state dynamics and cognitive flexibility in older adults. *Prog. Neurobiol.* **208**, 102180 (2022).
- Harrington, D. L. et al. Abnormal distraction and load-specific connectivity during working memory in cognitively normal Parkinson's disease. *Hum. Brain Mapp.* **41**, 1195–1211 (2020).
- Gerrits, N. J. et al. Compensatory fronto-parietal hyperactivation during set-shifting in unmedicated patients with Parkinson's disease. *Neuropsychologia* **68**, 107–116 (2015).
- Simioni, A. C., Dagher, A. & Fellows, L. K. Effects of levodopa on corticostriatal circuits supporting working memory in Parkinson's disease. *Cortex* **93**, 193–205 (2017).
- Trujillo, J. P. et al. Impaired planning in Parkinson's disease is reflected by reduced brain activation and connectivity. *Hum. Brain Mapp.* **36**, 3703–3715 (2015).
- Murphy, A. C., Bertolero, M. A., Papadopoulos, L., Lydon-Staley, D. M. & Bassett, D. S. Multimodal network dynamics underpinning working memory. *Nat. Commun.* **11**, 3035 (2020).

33. Finc, K. et al. Dynamic reconfiguration of functional brain networks during working memory training. *Nat. Commun.* **11**, 2435 (2020).
34. Cohen, J. R. & D'Esposito, M. The segregation and integration of distinct brain networks and their relationship to cognition. *J. Neurosci.* **36**, 12083–12094 (2016).
35. Braun, U. et al. Dynamic reconfiguration of frontal brain networks during executive cognition in humans. *Proc. Natl Acad. Sci.* **112**, 11678–11683 (2015).
36. Poston, K. L. et al. Compensatory neural mechanisms in cognitively unimpaired Parkinson disease. *Ann. Neurol.* **79**, 448–463 (2016).
37. Shakil, S., Lee, C.-H. & Keilholz, S. D. Evaluation of sliding window correlation performance for characterizing dynamic functional connectivity and brain states. *NeuroImage* **133**, 111–128 (2016).
38. Leonardi, N. & Van De Ville, D. On spurious and real fluctuations of dynamic functional connectivity during rest. *NeuroImage* **104**, 430–436 (2015).
39. Cai, W. et al. Latent brain state dynamics distinguish behavioral variability, impaired decision-making, and inattention. *Mol. Psychiatry* **26**, 4944–4957 (2021).
40. Menon, V. et al. Optogenetic stimulation of anterior insular cortex neurons in male rats reveals causal mechanisms underlying suppression of the default mode network by the salience network. *Nat. Commun.* **14**, 866 (2023).
41. Nair, A. et al. An approximate line attractor in the hypothalamus encodes an aggressive state. *Cell* **186**, 178–193.e115 (2023).
42. Altamura, M. et al. Dissociating the effects of Sternberg working memory demands in prefrontal cortex. *Psychiatry Res. Neuroimaging* **154**, 103–114 (2007).
43. Heinzl, S. et al. Neural correlates of training and transfer effects in working memory in older adults. *NeuroImage* **134**, 236–249 (2016).
44. Xu, J. et al. Altered dynamic functional connectivity in de novo Parkinson's disease patients with depression. *Front. Aging Neurosci.* **13**, 1029 (2022).
45. Navalpotro-Gomez, I. et al. Disrupted salience network dynamics in Parkinson's disease patients with impulse control disorders. *Parkinsonism Relat. Disord.* **70**, 74–81 (2020).
46. Matar, E. et al. Dynamic network impairments underlie cognitive fluctuations in Lewy body dementia. *npj Parkinson's Dis.* **8**, 16 (2022).
47. Fiorenzato, E. et al. Dynamic functional connectivity changes associated with dementia in Parkinson's disease. *Brain* **142**, 2860–2872 (2019).
48. Díez-Cirarda, M. et al. Dynamic functional connectivity in Parkinson's disease patients with mild cognitive impairment and normal cognition. *NeuroImage Clin.* **17**, 847–855 (2018).
49. Huse, D. M., Castelli-Haley, J., Orsini, L. S., Lenhart, G. & Abdalla, J. A. Patterns of initial pharmacotherapy for Parkinson's disease in the United States. *J. Geriatr. Psychiatry Neurol.* **19**, 91–97 (2006).
50. Roy, M.-A., Doiron, M., Talon-Croteau, J., Dupré, N. & Simard, M. Effects of antiparkinson medication on cognition in Parkinson's disease: a systematic review. *Can. J. Neurol. Sci.* **45**, 375–404 (2018).
51. Weber, M. A. et al. Quantifying the inverted U: a meta-analysis of prefrontal dopamine, D1 receptors, and working memory. *Behav. Neurosci.* **136**, 207 (2022).
52. Cools, R. et al. Role of dopamine and clinical heterogeneity in cognitive dysfunction in Parkinson's disease. *Prog. Brain Res.* **269**, 309–343 (2022).
53. Meder, D., Herz, D. M., Rowe, J. B., Lehericy, S. & Siebner, H. R. The role of dopamine in the brain-lessons learned from Parkinson's disease. *NeuroImage* **190**, 79–93 (2019).
54. Bishop, C. M. Pattern recognition and machine learning. *Springer. Google Sch.* **2**, 1122–1128 (2006).
55. Leijon, A. *Bayesian Learning of Gaussian mixtures: Variational" over-pruning" rRevisited* (KTH Royal Institute of Technology, 2013).
56. Murphy, K. P. *Probabilistic Machine Learning: Advanced Topics* (MIT Press, 2023).
57. Dance, H. & Paige, B. Fast and scalable spike and slab variable selection in high-dimensional Gaussian processes. In *International Conference on Artificial Intelligence and Statistics*, 7976–8002 (PMLR, 2022).
58. Lenore, K. & Greenberg, S. A. The geriatric depression scale (GDS). *AJN The American Journal of Nursing* **107**, 67–68 (2007).
59. Litvan, I. et al. Movement Disorders Society Scientific Issues Committee report: SIC Task Force appraisal of clinical diagnostic criteria for Parkinsonian disorders. *Mov. Disord.* **18**, 467–486 (2003).
60. Goetz, C. G. et al. Movement Disorder Society-sponsored revision of the Unified Parkinson's Disease Rating Scale (MDS-UPDRS): scale presentation and clinimetric testing results. *Mov. Disord.* **23**, 2129–2170 (2008).
61. Fan, L. et al. The human brainnetome atlas: a new brain atlas based on connectational architecture. *Cereb. Cortex* **26**, 3508–3526 (2016).
62. Wainwright, M. J. & Jordan, M. I. Graphical models, exponential families, and variational inference. *Found. Trends® Mach. Learn.* **1**, 1–305 (2008).
63. Jordan, M. I., Ghahramani, Z., Jaakkola, T. S. & Saul, L. K. An introduction to variational methods for graphical models. in *Learning in Graphical Models*, 105–161 (1998).
64. Hotelling, H. Relations between two sets of variates. In *Breakthroughs in Statistics: Methodology and Distribution*, 162–190 (Springer, New York, NY, 1992).
65. Smith, S. M. et al. A positive-negative mode of population covariation links brain connectivity, demographics and behavior. *Nat. Neurosci.* **18**, 1565 (2015).
66. Lee, B. et al. Dopaminergic modulation and dosage effects on brain state dynamics and working memory component processes in Parkinson's disease (Code). (2024). <https://doi.org/10.5281/zenodo.14567445>.

Acknowledgements

This research was supported by grants from the Stanford ADRC P50 AG047366 (K.L.P.), P30 AG066515 (V.W.H.), National Institute of Health EB022907 (V.M.), MH121069 (V.M.), NS086085 (V.M.), K99AG071837 (C.B.Y.), Alzheimer's Association AARFD-21-848178 (B.L.), AARFD-21-849349 (C.B.Y.), AARGD-NTF-21-850781 (W.C.), and generous support of the Scully Foundation and the John Blume Foundation.

Author contributions

Conceptualization: B.L., V.M.; Methodology: B.L., W.C., R.Y., V.M.; Data acquisition: K.L.P., S.R., J.K., L.Y., V.W.H.; Investigation: B.L.; Writing-original draft: B.L., V.M.; Writing-review and editing: B.L., C.B.Y., W.C., K.L.P., V.M.

Competing interests

The authors declare no competing interests.

Additional information

Supplementary information The online version contains supplementary material available at <https://doi.org/10.1038/s41467-025-56660-w>.

Correspondence and requests for materials should be addressed to Byeongwook Lee or Vinod Menon.

Peer review information *Nature Communications* thanks Nandakumar Narayanan, Kathrin Giehl, and Filip Grill for their contribution to the peer review of this work. A peer review file is available.

Reprints and permissions information is available at <http://www.nature.com/reprints>

Publisher's note Springer Nature remains neutral with regard to jurisdictional claims in published maps and institutional affiliations.

Open Access This article is licensed under a Creative Commons Attribution-NonCommercial-NoDerivatives 4.0 International License, which permits any non-commercial use, sharing, distribution and reproduction in any medium or format, as long as you give appropriate credit to the original author(s) and the source, provide a link to the Creative Commons licence, and indicate if you modified the licensed material. You do not have permission under this licence to share adapted material derived from this article or parts of it. The images or other third party material in this article are included in the article's Creative Commons licence, unless indicated otherwise in a credit line to the material. If material is not included in the article's Creative Commons licence and your intended use is not permitted by statutory regulation or exceeds the permitted use, you will need to obtain permission directly from the copyright holder. To view a copy of this licence, visit <http://creativecommons.org/licenses/by-nc-nd/4.0/>.

© The Author(s) 2025